Monitoring Landscape Dynamics via Multitemporal Classification at Comandante Ferraz Station neighborhood, Keller Peninsula, Antarctica.

Eduardo Soares Nascimento [1], Renato César dos Santos [2], Guilherme Pina Cardim [3], Samara Calçado de Azevedo [4], Pedro Pina [5], Erivaldo Antonio da Silva [2]

[1] Graduate Program in Cartographic Sciences (PPGCC), Department of Cartography, School of Technology and Sciences São Paulo State University (FCT-UNESP), 19060-900 Presidente Prudente, São Paulo, Brazil. (e.nascimento@unesp.br)

[2] Department of Cartography, School of Technology and Sciences São Paulo State University (FCT-UNESP), 19060-900 Presidente Prudente, São Paulo, Brazil. (renato.cesar, erivaldo.silva)@unesp.br

[3] Engineering Department, School of Engineering and Sciences São Paulo State University (FEC-UNESP), 19274-000, Rosana SP, Brazil. (guilherme.cardim@unesp.br)

[4] Institute of Natural Resources, Federal University of Itajubá (UNIFEI), 37500-903, Itajubá, MG, Brazil. (samara_calcado@unifei.edu.br)

[5] Department of Earth Sciences, Faculty of Sciences and Technology, University of Coimbra (UC), 3030-790, Coimbra, Portugal. (ppina@dct.uc.pt)

Keywords: Landscape dynamics, Comandante Ferraz Antarctic Station, Land Cover Change, Landsat, data cube, Random Forest.

Abstract

This study examines the landscape dynamics in the region surrounding Comandante Ferraz Antarctic Station, Keller Peninsula, King George Island, focusing on the quantification of land cover changes over 23 years. Emphasis is placed on the integration of a multitemporal Landsat time series (2001–2024) within a standardized spatio-temporal data cube framework, coupled with a Random Forest (RF) classification approach. This methodology enables consistent pixel-wise trajectory analysis across seven distinct epochs. The RF models achieved robust performance, with F1-scores for dominant classes like water and soil typically exceeding 0.90, although seasonal snow and ice showed greater spectral ambiguity in transitional months. Quantitative results from the transition matrices reveal a significant landscape reconfiguration: while ice (85.3%) and soil (81.2%) showed high persistence, a prominent trend of deglaciation was identified, characterized by the transition of ice and snow into exposed soil and the emergence of pioneer vegetation communities detected from 2014 onwards. The study demonstrates that the integration of machine learning and data cubes provides a powerful tool for monitoring environmental shifts in high-latitude maritime Antarctica, supporting long-term ecological assessments and climate impact modeling.

1. Introduction

Antarctica plays an essential role in regulating the global climate system (Simões et al., 2013). Over the past decades, the Antarctic Peninsula has undergone pronounced climatic shifts, with surface air temperatures rising at rates up to five times higher than the global average (Abram et al., 2025; Roland et al., 2024; Turner et al., 2020). These rapid changes have triggered significant landscape modifications, including glacier retreat, expansion of ice-free areas, and the proliferation of cryptogamic vegetation communities (Convey, 2006; Walshaw et al., 2024). Although permanently ice-free areas account for less than 0.5% of the Antarctic continent, they support nearly all terrestrial biodiversity and are highly sensitive to climatic fluctuations, making them key indicators of environmental change (Chown et al., 2015; Tóth et al., 2025).

King George Island, home to the Brazilian Comandante Ferraz Antarctic Station, has become a strategic site for monitoring cryospheric transformations in the maritime region. Multitemporal satellite analyses have revealed a reduction in glacier coverage of approximately 10% between 1989 and 2020, with marine-terminating glaciers exhibiting the highest rates of retreat. These changes are associated with regional warming trends and glacial-hydrogeomorphic processes, including the expansion of ice-free areas and meltwater lakes (da Rosa et al., 2023; Rojas-Macedo et al., 2024).

These findings highlight the need for methodological frameworks capable of quantifying and interpreting land cover dynamics in climatically sensitive regions such as the Antarctic Peninsula. In this context, remote sensing has proven indispensable, with the Landsat program providing multidecadal record for monitoring temporal analyses (Wulder et al., 2019). More recent missions, including Sentinel-2, have further advanced the capacity to detect vegetation patterns and subtle surface changes at higher spatial resolutions (Fonseca et al., 2023; Walshaw et al., 2024). However, despite the advantages of higher resolution sensors, a significant research gap remains regarding standardized, long-term monitoring frameworks that can bridge historical data with modern classification techniques in highly dynamic Antarctic zones.

Traditional vegetation indices, such as the Normalized Difference Vegetation Index (NDVI), have been widely applied to polar environments, but their effectiveness is limited by sparse vegetation cover, spectral confusion with exposed rocks, and the dominance of lichens and mosses (Calviño-Cancela & Martín-Herrero, 2016; King et al., 2020; Petsch et al., 2019; Pina et al., 2016)

To overcome these challenges, advanced classification approaches based on machine learning have gained prominence. In particular, Random Forest classifier has demonstrated high accuracy and robustness in heterogeneous environments, including polar ecosystems (Belgiu & Drăgu, 2016; Miranda et al., 2020; Sotille et al., 2022). Furthermore, the integration of multitemporal classifications into multidimensional data cubes enables systematic analyses of land cover transitions, facilitating the detection of long-term trends and abrupt shifts (Winkler et al., 2021).

This contribution has been peer-reviewed. The double-blind peer-review was conducted on the basis of the full paper.
https://doi.org/10.5194/isprs-annals-XI-3-2026-565-2026

This study focuses on the ice-free zones surrounding the Comandante Ferraz Antarctic Station, recognized as some of the most dynamic landscapes in maritime Antarctica. The selection of Landsat imagery for this study is justified by the requirement for a continuous and standardized historical record spanning over two decades, which remains a limitation for more recent high-resolution missions. To capture these spatiotemporal patterns, a multitemporal classification framework was proposed using imagery from 2001 to 2024. Random Forest classification, transition matrix analysis, and data cube structuring were integrated to characterize land cover dynamics and landscape evolution.

2. Methodology

2.1 Study Area

The study area encompasses the surroundings of Comandante Ferraz Station (62°05’S-58°23’W) on King George Island's Keller Peninsula. This zone features glaciers, meltwater lakes, periglacial landforms, and exposed terrain, undergoing rapid environmental changes. Its seasonal vegetation and surface variability make it an important site for monitoring land cover changes using remote sensing techniques (Figure 1).

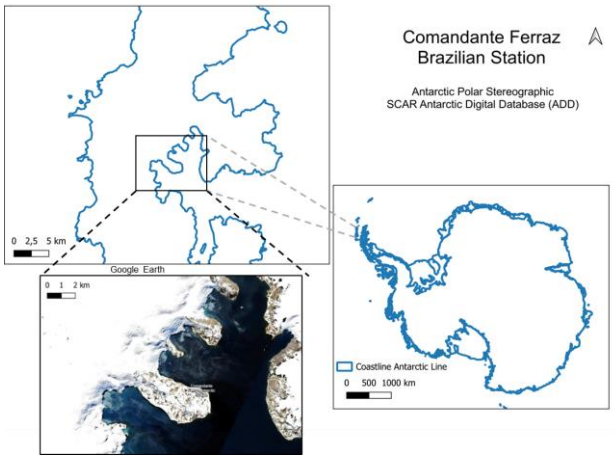

Figure 1. Study area contextualization: Comandante Ferraz Brazilian Station

2.2 Processing pipeline

The processing pipeline was designed to classify and analyse land cover changes in ice-free zones surrounding Comandante Ferraz Station using multitemporal Landsat imagery from 2001 to 2024. It integrates data preparation, classification, and post-analysis steps to ensure consistency and reproducibility. A summary of the proposed framework is illustrated in Figure 4.

i) Data preparation: Landsat scenes were selected with priority given to cloud-free conditions, which are essential for accurate surface classification. The Landsat Collection 2 Level 2 surface reflectance (SR) product was utilized, including imagery from Landsat 5 (TM), Landsat 7 (ETM+), and Landsat 8/9 (OLI/OLI-2). These products are pre-processed with atmospheric correction, ensuring consistency across the 23-year images.

Whenever possible, acquisitions were aligned with the austral summer period (from December to March) to minimize snow cover and maximize surface visibility. However, due to data availability constraints, some scenes from transitional seasons were included, provided they met the criteria for minimal cloud interference and acceptable surface exposure.

ii) Machine Learning applications: Random Forest was used for supervised classification of land cover (Breiman, 2001). The classification model was configured with 500 trees to ensure statistical stability and minimize generalization errors. Training samples were manually collected using QGIS software, based on visual interpretation of existing satellite imagery.

A stratified random sampling approach was adopted, totaling approximately 800 points per epoch. This technique was selected to ensure that all thematic classes, including those with restricted spatial distribution such as vegetation, were adequately represented within the training and validation datasets. The entire classification pipeline was implemented in Jupyter Notebook environment.

iii) Multitemporal cube creation: To enable pixel-wise temporal analysis, each thematic map resulting from Random Forest classification was spatially aligned and reclassified using standardized global class identifiers, as illustrated in Figure 2.

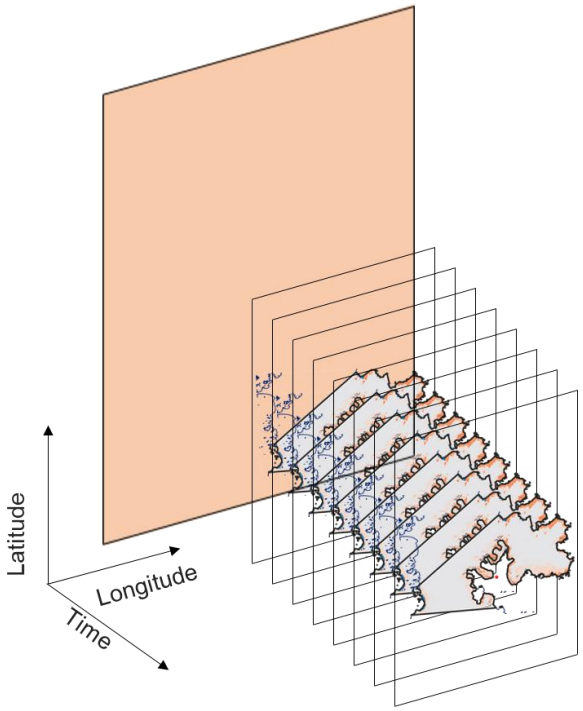

Figure 2. Illustration of data cube creation

Although vegetation was present in certain scenes, its absence in others was attributed to seasonal snow cover. Consequently, a unified global legend was established to encompass all observed classes (e.g., water, cloud, ice-free zones, ice, snow, and vegetation). Clouds were maintained as a specific class within this structure to preserve the spatial integrity of the data cube and to explicitly quantify obscured areas in each epoch. This approach was adopted to prevent the misinterpretation of visibility gains as actual land cover transitions.

Each map was subsequently reprocessed to match this global legend, ensuring spatial consistency across time. The final data cube was constructed by stacking the reclassified maps, allowing each pixel to retain its spatial identity while reflecting land cover changes over time. This structure enables temporal queries at the pixel level.

This contribution has been peer-reviewed. The double-blind peer-review was conducted on the basis of the full paper.
https://doi.org/10.5194/isprs-annals-XI-3-2026-565-2026 | © Author(s) 2026. CC BY 4.0 License.

iv) Multitemporal analysis: Transition matrices were computed for each pair of consecutive years. These matrices quantify the absolute and relative frequency of class changes, revealing key transformation pathways such as ice to soil, snow to water, and vegetation in previously barren areas. These results were exported as CSV tables for analysis and visualization.

The temporal stacking preserves the spatial identity of each pixel across all time slices. This structure allows class labels to be retrieved for any pixel through time, enabling detailed examination of land-cover trajectories—for instance, detecting pixels that shifted from ice to exposed soil throughout the study period (Figure 3).

v) Visualization and reporting: To support interpretation of land cover dynamics, graphical summaries were generated from the temporal data cube. Class proportions were calculated for each year and visualized using stacked bar charts and smoothed line plots. These visualizations highlight the relative distribution of classes such as water, ice, snow, vegetation, and exposed soil over time.

Subsequently, the corresponding values from selected spectral bands were extracted to form feature vectors (X_test), while reference class labels (y_test) were simultaneously retrieved from the annotated dataset. The trained Random Forest classifier was then applied to these test samples to generate predictions (y_pred). This procedure ensured that the evaluation was performed on independent data not utilized during the model training phase.

Model performance was rigorously evaluated by comparing predicted labels against the reference dataset, resulting in the generation of classification reports and confusion matrices for each epoch. Per-class metrics, including Precision, Recall, and F1-score, were computed and exported for each acquisition date to support a comparative analysis.

These metrics provided the statistical basis for assessing classification stability throughout the 23-year study period.

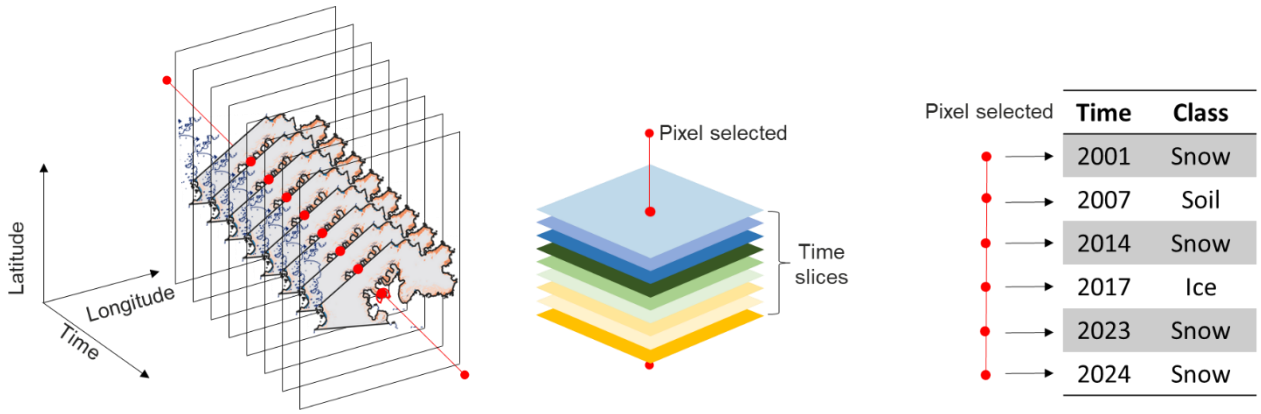

Figure 3. Multitemporal Analysis: pixel time transition

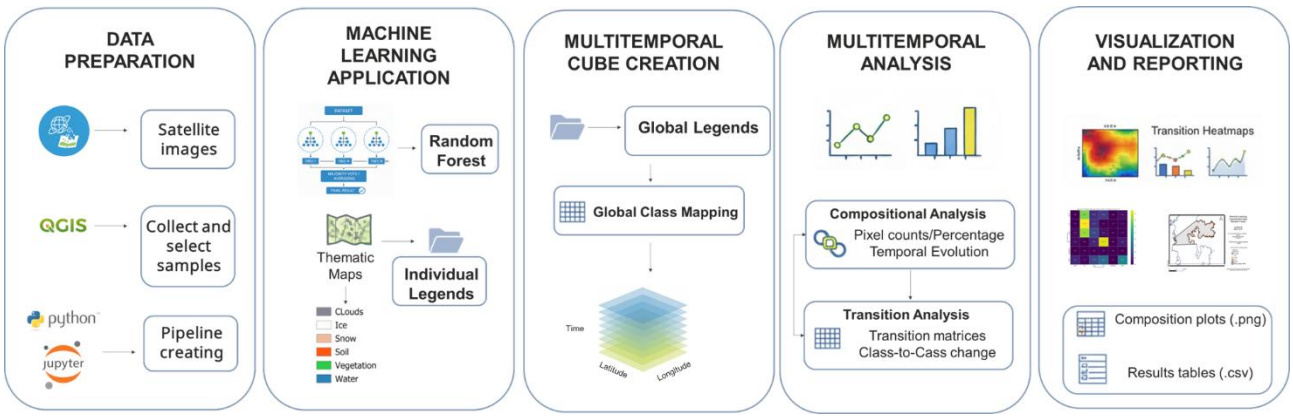

Figure 4. Proposed framework.

2.3 Quality analysis

The accuracy assessment was conducted through a structured process of data extraction and model evaluation using a multi-band geospatial raster stack. Ground-truth point data, stored in a GeoDataFrame, were used as a reference for sampling spectral information across the study area. For each reference point, geographic coordinates were converted into corresponding row and column indices to allow for precise pixel-level sampling.

3. Results

3.1 Classification performance

Table 1 presents the Precision, Recall, and F1-score values for each land cover class across all acquisition dates. These metrics were derived from the comparison between predicted labels and independent reference samples. Overall, the Random Forest model demonstrated high reliability, with dominant classes consistently achieving F1-scores above 0.90.

This contribution has been peer-reviewed. The double-blind peer-review was conducted on the basis of the full paper.
https://doi.org/10.5194/isprs-annals-XI-3-2026-565-2026 | © Author(s) 2026. CC BY 4.0 License.

Date	Class	Precision	Recall	F1-Score
2001-12-06	Ice	1.000	0.974	0.987
	Snow	0.809	0.905	0.854
	Soil	0.872	0.791	0.829
	Water	0.973	0.973	0.973
	Clouds	1.000	1.000	1.000
2007-01-14	Ice	1.000	1.000	1.000
	Snow	1.000	0.976	0.988
	Soil	0.944	0.985	0.964
	Water	0.981	0.944	0.962
2014-01-16	Water	0.980	0.926	0.952
	Clouds	0.583	0.724	0.646
	Vegetation	0.735	0.625	0.676
	Ice	0.875	0.800	0.836
	Snow	0.917	1.000	0.957
	Soil	0.952	1.000	0.976
2014-09-29	Water	0.811	0.833	0.822
	Clouds	0.925	0.881	0.902
	Ice	0.710	0.579	0.638
	Snow	0.545	0.667	0.600
	Soil	0.929	1.000	0.963
2017-03-06	Water	0.895	0.850	0.872
	Clouds	0.825	1.000	0.904
	Vegetation	0.821	0.657	0.730
	Ice	0.784	0.870	0.825
	Snow	0.852	0.742	0.793
	Soil	0.941	0.889	0.914
2021-01-12	Water	1.000	1.000	1.000
	Clouds	0.912	0.861	0.886
	Vegetation	0.778	0.875	0.824
	Ice	0.636	0.618	0.627
	Snow	0.828	0.706	0.762
	Soil	0.933	1.000	0.966
2023-09-06	Ice	0.711	0.800	0.753
	Snow	0.775	0.721	0.747
	Soil	0.759	0.759	0.759
	Water	0.981	0.945	0.963
2024-12-07	Ice	0.900	0.730	0.806
	Snow	0.738	0.816	0.775
	Soil	0.725	0.784	0.753
	Water	0.980	0.962	0.971
	Clouds	0.984	1.000	0.992

Table 1. Quality metrics for individual classes using data acquired at different epochs.

3.2 Land cover transitions

Transition matrices were computed for each pair of consecutive years to quantify landscape dynamics over the study period. The absolute and relative frequencies of land cover changes were quantified, and the complete set of matrices was structured for temporal comparison, capturing transitions such as ice to soil, snow to water, and vegetation. To exemplify the classification results, two thematic maps are shown - one corresponding to the year 2001 and another to 2024 - representing the initial and final states of the study period (Figures 5 and 6, respectively).

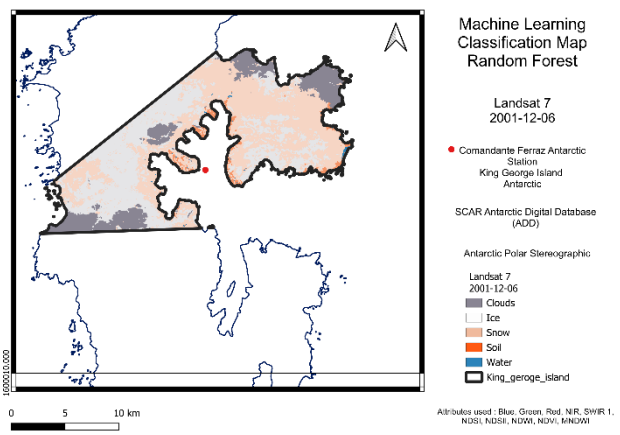

Figure 5. Classification Map: 2001-12-06

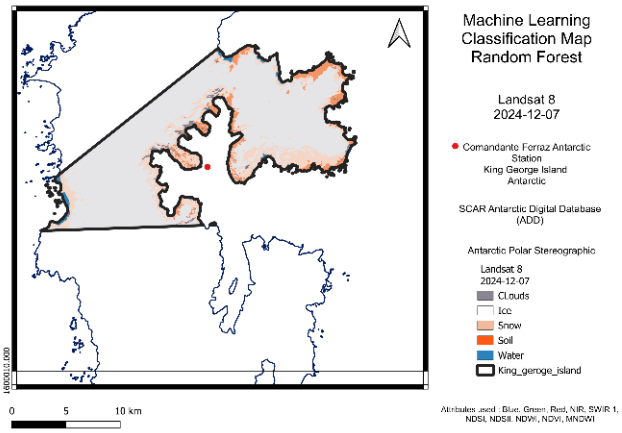

Figure 6. Classification Map: 2024-12-07

A heatmap was subsequently created to illustrate the intensity and spatial distribution of transitions over the entire time period (Figure 7). The Transition Matrix is normalized by row, with each cell representing the percentage proportion of the area of the origin class (2001) that transitioned into the destination class (2024). The sum of all values in each row equals 100%, allowing for a standardized interpretation of class shifts. This structure enables the direct quantification of landscape stability, represented by the values along the diagonal, and the area of transition, indicated by the values outside the diagonal. For instance, the value in the "Ice to Soil" cell directly quantifies the proportion of glacier area that has been lost to ice-free zones, providing a clear numerical metric for deglaciation processes.

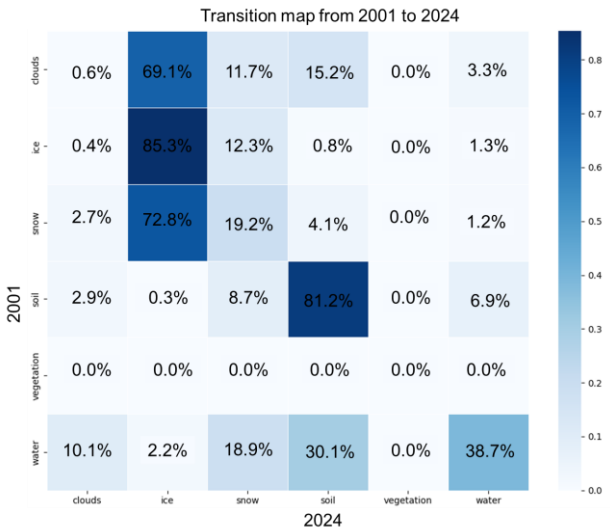

Figure 7. Heatmap (from 2001-12-06 to 2024-12-07)

Additionally, the frequency of each land cover class over time was analyzed using a graphical stacked bar chart representation (Figure 8). This visualization allows for the identification of seasonal trends and long-term fluctuations in surface components, such as the progressive increase in exposed soil relative to snow-covered areas.

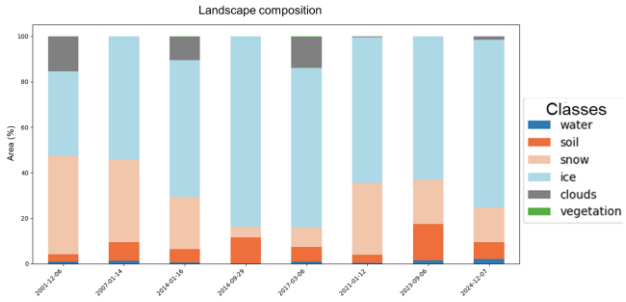

Figure 8. Frequency of each land cover class over time

4. Discussions

4.1 Classification performance

The classification metrics presented in Table 1 reveal consistent performance for dominant classes such as water and soil. High Precision and Recall were maintained across all acquisition dates, suggesting strong spectral separability and stable surface conditions, particularly during summer scenes.

In contrast, classes like ice and snow exhibited greater variability, specifically in transitional months (September and March). Lower F1-scores in these periods are attributed to spectral ambiguity, mixed pixels, and seasonal overlap between snow and ice-covered surfaces. For example, on 2014-09-29, a F1-score of 0.60 was achieved for snow, while ice dropped to 0.64, highlighting classification challenges under transitional illumination and surface conditions.

The appearance of vegetation from 2014 onwards introduced additional complexity. Despite its minimal representation (>0.05%), reasonable performance was achieved, with F1-scores ranging from 0.68 to 0.82. This reflects the sparse and heterogeneous distribution of vegetation in ice-free zones, which remains a challenge for 30 m resolution sensors.

4.2 Land cover dynamics

The classification outputs for the years 2001 and 2024 are illustrated in Figures 5 and 6. In the 2001 scene, extensive cloud cover was detected over coastal regions, leading to increased uncertainty and a reduction in recall for the soil class. Conversely, the 2024 scene was acquired under near cloud-free conditions, allowing for more accurate delineation of land cover types.

As indicated by the total class transition matrix (Figure 7), high rates of stability were observed for ice (85.3%) and soil (81.2%), suggesting that large portions of the interior zones remained unchanged. However, significant transitions from ice to soil and snow to soil were identified, reinforcing the trend of glacial retreat. Lower persistence was noted for water (38.7%), which is influenced by seasonal meltwater dynamics and hydrological shifts.

The temporal variation in landscape composition is depicted in Figure 8. A gradual expansion of exposed soil was identified in later dates, accompanied by a progressive decrease in snow coverage from November to February. Vegetation was detected in increasing proportions during peak summer conditions, suggesting a correlation between biological activity and the expansion of ice-free zones.

4.3 Environmental Implications

The observed land cover transitions around Comandante Ferraz Station reflect significant environmental dynamics over the 23 years. The progressive retreat of ice and snow, as evidenced by the transition matrices and temporal graphs, suggests a pattern of deglaciation consistent with broader climatic trends in the Antarctic Peninsula region. The increase in soil and vegetation coverage, particularly in coastal and periglacial zones, indicates that formerly glaciated areas are becoming increasingly exposed and biologically active.

Cloud cover, particularly in earlier acquisitions such as 2001, may have obstructed key features of the exposed terrain. This limitation underscores the importance of selecting optimal imagery for long-term monitoring and reinforces the need for complementary data sources, such as UAV (Unmanned Aerial Vehicle) surveys or very-high-resolution sensors (metric scale like WorldView), to validate these 30 m satellite-based classifications.

Overall, the documented transformations suggest that the Keller Peninsula is undergoing active landscape reconfiguration, with implications for geomorphology, ecology, and climate adaptation. Continued monitoring of these dynamics is essential for assessing the trajectory of environmental change and informing conservation strategies in Antarctic ice-free zones.

4.4 Limitations

Despite the robustness of the classification pipeline and the integration of multitemporal analysis, several limitations were identified throughout the study:

Cloud interference: As observed in the 2001 scene (Figure 5), extensive cloud cover over coastal regions likely obstructed key surface features, particularly ice-free zones. This limitation may have reduced the model’s ability to correctly identify soil and vegetation, impacting the recall of these classes and introducing uncertainty in early-stage land cover estimates. Additionally, shaded areas—caused by topographic relief or cloud shadows—were occasionally misclassified as clouds, further complicating the accurate delineation of surface classes in regions with complex illumination.

Seasonal variability: Although priority was given to summer acquisitions, some scenes were obtained during transitional periods due to data availability constraints. These conditions—characterized by mixed snow/ice surfaces and variable illumination—may have contributed to spectral ambiguity and reduced classification accuracy, especially for ice and snow classes.

Training sample subjectivity: The manual collection of training samples through visual interpretation introduces a degree of subjectivity. While care was taken to ensure representative sampling, subtle mislabeling or inconsistent boundaries may have influenced model performance, particularly in heterogeneous zones.

Vegetation detection: The sparse and patchy nature of Antarctic vegetation, combined with its low spectral contrast against surrounding terrain, poses challenges for remote sensing classification. Although vegetation was detected from 2014 onward, its representation remains limited and may be underestimated due to resolution constraints and spectral mixing confusion.

This contribution has been peer-reviewed. The double-blind peer-review was conducted on the basis of the full paper.
https://doi.org/10.5194/isprs-annals-XI-3-2026-565-2026 | © Author(s) 2026. CC BY 4.0 License.

Spatial resolution: Landsat imagery, while suitable for regional analysis, may not capture fine-scale features such as narrow meltwater channels, small vegetation patches, or microtopographic variations. These limitations affect the granularity of detected transitions and may overlook localized dynamics.

Temporal gaps: The temporal spacing between acquisitions varies, with some years lacking suitable imagery. This irregularity may hinder the detection of short-term transitions or seasonal reversals, limiting the continuity of change trajectories.

These limitations should be considered when interpreting the results and underscore the importance of integrating complementary data sources and higher-resolution imagery in future studies.

5. Conclusion

In this study, land cover dynamics in the vicinity of Comandante Ferraz Station were investigated using multitemporal Landsat imagery and supervised classification based on the Random Forest algorithm. A processing pipeline was proposed to ensure spatial consistency, temporal comparability, and reproducibility across the 2001–2024 period.

Consistent patterns of environmental transformation were revealed through transition matrices, with deglaciation and surface exposure being evidenced by transitions from ice to soil. The emergence of vegetation in later years suggests ecological expansion in newly ice-free zones, reinforcing the importance of long-term monitoring.

Future work may focus on integrating the current pipeline with radar data to improve temporal resolution and overcome limitations caused by cloud cover. The application of deep learning models could also be explored to enhance classification accuracy, particularly in spectrally complex or transitional areas. Additionally, incorporating in situ data would be essential for validating classification outputs, increasing the reliability of land cover assessments, and supporting more robust environmental interpretations.

Acknowledgements

This study was financed, in part, by the São Paulo Research Foundation (FAPESP), Brazil. Process Numbers: 2023/16874-1 and 2025/13513-3.

References

Abram, N. J., Purich, A., & England, M. H. (2025). Emerging evidence of abrupt changes in the Antarctic environment. *Nature*, *644*(8077), 621–633. https://doi.org/10.1038/s41586-025-09349-5

Belgiu, M., & Drăgu, L. (2016). Random forest in remote sensing: A review of applications and future directions. *ISPRS Journal of Photogrammetry and Remote Sensing*, *114*, 24–31. https://doi.org/10.1016/J.ISPRSJPRS.2016.01.011

Breiman, L. (2001). *Random Forests*. *45*, 5–32.

Calviño-Cancela, M., & Martín-Herrero, J. (2016). Spectral Discrimination of Vegetation Classes in Ice-Free Areas of Antarctica. *Remote Sensing*, *8*(10), 856. https://doi.org/10.3390/rs8100856

Chown, S. L., Clarke, A., Fraser, C. I., Cary, S. C., Moon, K. L., & McGeoch, M. A. (2015). The changing form of Antarctic biodiversity. *Nature*, *522*(7557), 431–438. https://doi.org/10.1038/nature14505

Convey, P. (2006). Antarctic climate change and its influences on terrestrial ecosystems. *Trends in Antarctic Terrestrial and Limnetic Ecosystems: Antarctica as a Global Indicator*, 253–272.

da Rosa, K. K., Perondi, C., Lorenz, J. L., Auger, J. D., Cazaroto, P., Petsch, C., Siqueira, R. G., Simões, J. C., & Vieira, R. (2023). Glacier fluctuations and a proglacial evolution in King George Bay (King George Island), Antarctica, since 1980 decade. *Anais Da Academia Brasileira de Ciências*, *95*, e20230624. https://doi.org/10.1590/0001-3765202320230624

Fonseca, E. L. da, Santos, E. C. dos, Figueiredo, A. R. de, & Simões, J. C. (2023). The use of sentinel-2 imagery to generate vegetations maps for the Northern Antarctic peninsula and offshore islands. *Anais Da Academia Brasileira de Ciências*, *95*(suppl 3), e20230710. https://doi.org/10.1590/0001-3765202320230710

King, D. H., Wasley, J., Ashcroft, M. B., Ryan-Colton, E., Lucieer, A., Chisholm, L. A., & Robinson, S. A. (2020). Semi-Automated Analysis of Digital Photographs for Monitoring East Antarctic Vegetation. *Frontiers in Plant Science*, *11*, 521828. https://doi.org/10.3389/FPLS.2020.00766/BIBTEX

Miranda, V., Pina, P., Heleno, S., Vieira, G., Mora, C., & E.G.R. Schaefer, C. (2020). Monitoring recent changes of vegetation in Fildes Peninsula (King George Island, Antarctica) through satellite imagery guided by UAV surveys. *Science of The Total Environment*, *704*, 135295. https://doi.org/10.1016/j.scitotenv.2019.135295

Petsch, C., Costa, R. M., da Rosa, K. K., Vieira, R., & Simões, J. C. (2019). Identificação e mapeamento em mesoescala da zona proglacial da Geleira Collins, Ilha Rei George, Antártica. *Quaternary and Environmental Geosciences*, *10*(1/2).

Pina, P., Vieira, G., Bandeira, L., & Mora, C. (2016). Accurate determination of surface reference data in digital photographs in ice-free surfaces of Maritime Antarctica. *Science of The Total Environment*, *573*, 290–302. https://doi.org/10.1016/J.SCITOTENV.2016.08.104

Rojas-Macedo, I., Bello, C., Suarez, W., Loarte, E., Vega-Jacome, F., Bustamante Rosell, M. G., & Tapia, P. M. (2024). Using satellite imagery to assess glacier retreat in King George Island, Antarctica. *Revista de Teledeteccion*, *2024*(65). https://doi.org/10.4995/RAET.2025.22317

Roland, T. P., Bartlett, O. T., Charman, D. J., Anderson, K., Hodgson, D. A., Amesbury, M. J., Maclean, I., Fretwell, P. T., & Fleming, A. (2024). Sustained greening of the Antarctic Peninsula observed from satellites. *Nature Geoscience*, *17*(11), 1121–1126. https://doi.org/10.1038/s41561-024-01564-5

Simões, J. C., Viana, A. R., Secchi, E. R., Correia, E., Silva, H. E. da, Wainer, I. E. K. C., Campos, L. de S., Mata, M. M., Pelizzari, V. H., & Valentin, Y. Y. (2013). Antartic science for Brazil : an action plan for the 2013-2022 period. *Repositório Digital- MINISTÉRIO DA CIÊNCIA, TECNOLOGIA E INOVAÇÃO*, 36.

Sotille, M. E., Bremer, U. F., Vieira, G., Velho, L. F., Petsch, C., Auger, J. D., & Simões, J. C. (2022). UAV-based classification of maritime Antarctic vegetation types using GEOBIA and random forest. *Ecological Informatics*, *71*, 101768. https://doi.org/10.1016/j.ecoinf.2022.101768

Tóth, A. B., Terauds, A., Chown, S. L., Hughes, K. A., Convey, P., Hodgson, D. A., Cowan, D. A., Gibson, J., Leihy, R. I.,

Murray, N. J., Robinson, S. A., Shaw, J. D., Stark, J. S., Stevens, M. I., van den Hoff, J., Wasley, J., & Keith, D. A. (2025). A dataset of Antarctic ecosystems in ice-free lands: classification, descriptions, and maps. *Scientific Data*, *12*(1), 133. https://doi.org/10.1038/s41597-025-04424-y

Turner, J., Guarino, M. V., Arnatt, J., Jena, B., Marshall, G. J., Phillips, T., Bajish, C. C., Clem, K., Wang, Z., Andersson, T., Murphy, E. J., & Cavanagh, R. (2020). Recent Decrease of Summer Sea Ice in the Weddell Sea, Antarctica. *GeoRL*, *47*(11), e87127. https://doi.org/10.1029/2020GL087127

Walshaw, C. V., Gray, A., Fretwell, P. T., Convey, P., Davey, M. P., Johnson, J. S., & Colesie, C. (2024). A satellite-derived baseline of photosynthetic life across Antarctica. *Nature Geoscience*, *17*(8), 755–762. https://doi.org/10.1038/s41561-024-01492-4

Winkler, K., Fuchs, R., Rounsevell, M., & Herold, M. (2021). Global land use changes are four times greater than previously estimated. *Nature Communications*, *12*(1), 2501. https://doi.org/10.1038/s41467-021-22702-2

Wulder, M. A., Loveland, T. R., Roy, D. P., Crawford, C. J., Masek, J. G., Woodcock, C. E., Allen, R. G., Anderson, M. C., Belward, A. S., Cohen, W. B., Dwyer, J., Erb, A., Gao, F., Griffiths, P., Helder, D., Hermosilla, T., Hipple, J. D., Hostert, P., Hughes, M. J., … Zhu, Z. (2019). Current status of Landsat program, science, and applications. *Remote Sensing of Environment*, *225*, 127–147. https://doi.org/10.1016/J.RSE.2019.02.015